



ORIGINAL ARTICLE

Biology-oriented drug synthesis of nitrofurazone derivatives: Their α -glucosidase inhibitory activity and molecular docking studies



Sana Wahid^a, Sajid Jahangir^a, Muhammad Ali Versiani^a,
Khalid Mohammed Khan^{b,c,*}, Yeong Yik Sung^{h,*}, Jamshed Iqbal^d,
Abdul Wadood^e, Kanwal^{b,h}, Ashfaq Ur Rehman^{e,i}, Arshia^b, Muhammad Uzair^d,
Imtiaz Ali Khan^d, Muhammad Taha^c, Shahnaz Perveen^g

^a Department of Chemistry, Federal Urdu University of Art, Science, and Technology, Karachi, Pakistan

^b H. E. J. Research Institute of Chemistry, International Center for Chemical and Biological Sciences, University of Karachi, Karachi 75270, Pakistan

^c Department of Clinical Pharmacy, Institute for Research and Medical Consultations (IRMC), Imam Abdulrahman Bin Faisal University, P.O. Box 31441, Dammam, Saudi Arabia

^d Centre for Advanced Drug Research, COMSATS University Islamabad, Abbottabad Campus, Abbottabad 22060, Pakistan

^e Department of Biochemistry, Computational Medicinal Chemistry Laboratory, UCSS, Abdul Wali Khan University Mardan, Khyber Pakhtunkhwa 23200, Pakistan

^g PCSIR Laboratories Complex, Karachi, Shahrah-e-Dr. Salimuzzaman Siddiqui, Karachi 75280, Pakistan

^h Institute of Marine Biotechnology, Universiti Malaysia Terengganu, 21030 Kuala Terengganu, Terengganu, Malaysia

ⁱ Department of Molecular Biology and Biochemistry, University of California, Irvine, CA 92697-3900, United States

Received 18 November 2021; accepted 16 February 2022

Available online 23 February 2022

KEYWORDS

Nitrofurazone;
Diabetes;
In silico studies;
 α -glucosidase inhibition

Abstract In the present study, twenty (20) structural variants of nitrofurazone were synthesized based on BIODS (Biology-oriented drug synthesis) approach. The structure elucidation of the synthetic molecules (1–20) was carried out using different spectroscopic techniques, and their α -glucosidase inhibitory activity was also determined. The synthetic molecules 1–20 exhibited good α -glucosidase inhibition than the parent, nitrofurazone. Four compounds 2, 4, 6, and 7 showed potential inhibition against α -glucosidase with IC₅₀ values ranging between 0.63 ± 0.25–1.29 ± 0.

* Corresponding authors.

E-mail addresses: khalid.khan@iccs.edu (K. Mohammed Khan), yeong@umt.edu.my (Y. Yik Sung).

Peer review under responsibility of King Saud University.



46 μM as compared to the standard acarbose ($\text{IC}_{50} = 2.05 \pm 0.41 \mu\text{M}$). Nevertheless, compounds **15** ($\text{IC}_{50} = 0.74 \pm 0.12 \mu\text{M}$), and **19** ($\text{IC}_{50} = 0.54 \pm 0.3 \mu\text{M}$) also displayed good α -glucosidase inhibition and compound **19** was the most active compound of the series. Kinetic study of the active compounds **7** and **19** was also carried out to confirm the mode of inhibition. The binding interactions of the most active compounds within the active site of enzyme were determined by molecular docking. Moreover, molecular dynamic simulation of compound **19** was also performed in order to determine the stability of the overall complex (α -glucosidase + c19) in an explicit watery environment. The synthetic molecules were predicted as non-cytotoxic, however, seven compounds **1**, **3**, **4**, **9**, **10**, **11**, and **12** were predicted as carcinogenic.

© 2022 The Authors. Published by Elsevier B.V. on behalf of King Saud University. This is an open access article under the CC BY-NC-ND license (<http://creativecommons.org/licenses/by-nc-nd/4.0/>).

1. Introduction

α -Glucosidase belongs to the family of hydrolase enzymes and contains calcium as a metal atom. The primary purpose of this enzyme is to degrade glycogen into glucose in lysosomes. However, it is responsible for the increased blood glucose level in type-2 diabetes mellitus. Therefore, it is quite necessary to target and inhibit the excess activity of this enzyme to control diabetes. The compounds capable of inhibiting the intestinal α -glucosidase enzyme usually slow down the digestion and absorption of carbohydrates. Thus, meal-related hyperglycemia can be controlled through these inhibitors. Moreover, the inhibition of α -glucosidase has a profound effect on the glycan structure which consequently affects the maturation, transport, secretion, and function of glycoproteins (Nashiru et al., 2001; Park et al., 2008; Bosenberg and Van Zyl, 2008; Abbasi et al., 2017; Davies and Henrissat, 1995; Van de Laar, 2008; Azam et al., 2012). Several α -glucosidase inhibitors have been reported in the literature, such as acarbose, nojirimycin, 1-deoxynojirimycin, miglitol, and voglibose (Bosenberg and Van Zyl, 2008; Khan et al., 2014; Liu et al., 2006). The α -glucosidase inhibitors can effectively treat diabetes and other clinical conditions that are carbohydrate mediated, such as cancer, obesity, hepatitis, and hyperlipoproteinemia (de Melo et al., 2006; Fischer et al., 1995). According to the World Health Organization, the number of type 2 diabetic cases will reach 360 million by 2030. The goal of diabetes treatment is to control blood glucose levels, particularly after a meal, obesity, cholesterol, and triglyceride levels, as well as to predict the progression of complications (Yoshikawa et al., 2010).

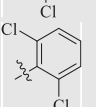
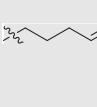
Biology-oriented drug synthesis is focused on the chemical transformation and modification of commercially available drugs to create the libraries of compounds that can serve as lead molecules and might be evaluated for their diversified biological properties (Khan et al., 2018). During past years, our group has targeted and synthesized several libraries of compounds based on commercial drugs under the umbrella of biology-oriented syntheses. The synthetic molecules were found to possess diversified biological activities i.e. flurbiprofen derivatives were reported as novel α -amylase inhibitors (Yoshikawa et al., 2010); S-naproxen derivatives were found to have potential urease inhibitory activity (Mohiuddin et al., 2019); metronidazole derivatives showed good β -glucuronidase and α -amylase inhibitory activities (Muhammad et al., 2017), piroxicam derivatives were also reported for their antinociceptive activity (Ullah et al., 2016),

and atenolol derivatives were also reported as urease inhibitors (Wahid et al., 2020). In continuation of our research on biology-oriented drug synthesis (BIODS), we had targeted another commercially available drug nitrofurazone to synthesize a library of compounds and evaluated their α -glucosidase inhibitory activity.

Nitrofurazone is available commercially with the trade name of furacin (Ullah et al., 2016) and is the first 5-NO₂-furan medicine (Brito et al., 2013) approved as an antichagasic drug regardless of its toxicity. The causative agent of this disease is *Trypanosoma cruzi*, commonly found in Latin America and was responsible for almost 25 million deaths in 2008. Nitrofurazone has shown antitrypanosomal activity by inhibiting a specific parasite detoxifying enzyme trypanothione reductase. It is also known to inhibit the parasite protease i.e., cruzipain. The mechanistic action of nitrofurazone is still not fully understood, however, it has a wide range of activities against different organisms including parasites and bacteria (Chin Chung et al., 2011; Blumenstiel et al., 1999; Paulino et al., 2005). Nitrofurazone also possesses a wide spectrum of antimicrobial properties and is effective against both Gram-positive and Gram-negative bacterial strains. Nitrofurazones are found to be effective against trypanosomes (Chamberlain, 1976). Nitrofurazone and its analogs are found to be active against *Staphylococcus* spp. ATTC and *Bacillus* spp. ATTC (Popiołek and Biernasiuk, 2016).

In our previous work, we demonstrated the synthesis and antidiabetic activities of different classes of compounds namely indoles, oxadiazoles, hydrazides, etc. (Taha et al., 2017; Khan et al., 2018; Gollapallia et al., 2018; Abbasi et al., 2017). Fig. 1 represents the classes of compounds that were found to have α -glucosidase and α -amylase inhibitory activities, though the parent moieties of these compounds are different, these compounds have few structural similarities i.e. presence of amide linkage. Keeping that in mind, we have modified the nitrofurazone molecule by treating it with different substituted *N*-alkyl/aryl derivatives to afford synthetic molecules **1–20** and screened them for α -glucosidase inhibitory activity (Figure-1 in Supp. inf.). Compounds **1–20** were synthesized using eight alkyl bromides and twelve benzyl chlorides. Out of the synthesized compounds, compounds **1–12**, and **16–20** are newly synthesized while compounds **13–19**, and **17** are already reported in the literature (Tocher, 1997; Brondani et al., 2007; Bartel et al., 2009). Thus, this study reports the synthesis of nitrofurazone derivatives **1–20** and the *in vitro* α -glucosidase inhibitory activities along with the *in silico* study to confirm the binding interactions of compounds within the enzyme pocket.

Table 1 IC₅₀ values of nitrofurazone derivatives (1–20) against α glucosidase enzyme.

| C. No. | R | IC ₅₀ ± SEM (μM) | C. No. | R | IC ₅₀ ± SEM (μM) |
|----------------------|---|-----------------------------|--|---|-----------------------------|
| 1 |  | 17.2 ± 3.21 | 11 |  | 34.3 ± 3.38 |
| 2 |  | 1.29 ± 0.46 | 12 |  | 1.24 ± 0.38 |
| 3 |  | 28.1 ± 1.34 | 13 |  | 12.7 ± 5.38 |
| 4 |  | 0.63 ± 0.25 | 14 |  | 20.2 ± 1.21 |
| 5 |  | 12.4 ± 1.54 | 15 |  | 0.74 ± 0.12 |
| 6 |  | 0.63 ± 0.25 | 16 |  | 28.4 ± 2.11 |
| 7 |  | 0.65 ± 0.22 | 17 |  | 30.9 ± 3.21 |
| 8 |  | 14.2 ± 0.93 | 18 |  | 24.0 ± 2.12 |
| 9 |  | 1.63 ± 0.28 | 19 |  | 0.54 ± 0.30 |
| 10 |  | 37.1 ± 2.09 | 20 |  | 27.3 ± 1.56 |
| Nitrofurazone | | 37.5 ± 2.87 | Standard^b = Acarbose | | 2.05 ± 0.41 |

SEM^a (Mean ± Standard error of the mean); Standard^b (Inhibitor for α -glucosidase activity).

groups was less active in comparison with other molecules of similar type (Figure-6 in Supp. inf.).

Among methyl and methoxy substituted compounds **10** (IC₅₀ = 37.1 ± 2.09 μM), **11** (IC₅₀ = 34.3 ± 3.38 μM), and **12** (IC₅₀ = 1.24 ± 0.38 μM), compound **12** with methoxy group at *meta* position displayed potential inhibition against the α -glucosidase enzyme, might be due to the inductive effect of methoxy group present at *meta* position (Figure-7 in Supp. inf.).

2.5. Category B

This category comprises of total eight compounds **13–20**. Among them, compounds **15** (IC₅₀ = 0.74 ± 0.12 μM) and **19** (IC₅₀ = 0.54 ± 0.30 μM) displayed good inhibitory activities as compared to the standard acarbose. Compound **19** was discovered to be the most active of the series, which suggests that the octyl chain attached to the nitrofurazone has achieved a configuration that fits into the enzyme's active site. However, compound **15** with pentyl chain also displayed good inhibition but was less active than compound **19** of nitrofurazone derivatives (Figure-8 in Supp. inf.).

2.6. Enzyme kinetics study for α -glucosidase inhibition

Enzyme kinetics studies were performed to find out the mode of enzyme inhibition. The most potent compounds **7** and **19** among the tested ones were selected for kinetic studies. Both

the compounds were used at a concentration of 0, 0.3, 0.6, and 0.9 μM. Compound **7** showed competitive inhibition while compound **19** revealed uncompetitive inhibition against α -glucosidase (Figure-9 in Supp.inf.).

2.7. Molecular docking study

A molecular docking study was performed to further understand the binding mode of all synthesized compounds against the α -glucosidase enzyme. The lead compound nitrofurazone results (Figure-10 in Supp. inf.) were compared with all the top conformations from each compound and were found in a well-accommodated pattern in the active site of the enzyme, except compound **20**, which hold a much bulky group, this compound was found much bigger than the radius of the active site, which unable to accommodate well, also adopted π -stacking interactions with some local residues. While other active compounds in the series showed numerous key interactions with active site residues that might play important role in the enhancement of enzymatic activity. The details of the protein–ligand interaction profile have been enlisted in Table 2. Moreover, the docking results of the standard lead compound revealed key interactions with the active site residues, comparatively, it has been observed that the docking results of our enlisted compounds are far better than the standard compound.

We have enlisted the synthetic compounds into two categories based on the substituted groups, category-A bearing the benzene (aryl) substitution, while Category-B holds the

Table 2 Docking scores and report of predicted interactions of docked conformations against the α -glucosidase enzyme.

| C. No. | Interaction details | | | | | | Docking score (S) |
|--------|---------------------|----------|---------------|----------|-----------|---------|-------------------|
| | Ligands | Receptor | | Distance | E cal/mol | residue | |
| NFZ | O | OH | H-accepter | 2.63 | -2.3 | TYR344 | -8.2098 |
| 1 | N1 | OD2 | H-donor | 4.14 | -1.8 | ASP349 | -9.0991 |
| | N5 | 6-ring | π -H | 4.34 | -0.8 | TYR71 | |
| 2 | C15 | OD2 | H-donor | 2.84 | -0.1 | ASP349 | -10.8071 |
| | N2 | ND2 | H-accepter | 3.49 | -0.1 | ASN347 | |
| | O4 | CE1 | H-accepter | 2.44 | -0.1 | HIS348 | |
| | O13 | CA | H-accepter | 3.18 | -0.5 | PHE300 | |
| 3 | C15 | OD2 | H-donor | 3.12 | -0.5 | ASP349 | -9.0012 |
| 4 | CL22 | OE2 | H-donor | 4.05 | -0.3 | GLU304 | -9.2390 |
| | O14 | CB | H-accepter | 2.91 | -0.1 | PHE177 | |
| | CL22 | CB | H-accepter | 3.30 | -0.1 | PHE300 | |
| | 6-ring | CD | π -H | 4.23 | -0.5 | ARG312 | |
| 5 | N1 | OE4 | H-donor | 2.89 | -9.4 | GLU276 | -10.5777 |
| | O4 | ND2 | H-accepter | 3.23 | -2.2 | ASN347 | |
| 6 | N5 | ODI | H-donor | 2.16 | -3.1 | ASN347 | -11.7045 |
| | O14 | NH1 | H-donor | 2.71 | -0.1 | ARG439 | |
| | O4 | ND2 | H-accepter | 1.79 | -4.1 | ASN347 | |
| | Cl23 | CD | H-accepter | 2.84 | -3.8 | ARG439 | |
| 7 | C15 | OD1 | H-donor | 3.03 | -1.2 | ASP214 | -11.5945 |
| | O4 | NH2 | H-accepter | 2.93 | -0.3 | ARG212 | |
| | O4 | NE2 | H-accepter | 2.53 | -3.6 | HIS348 | |
| | O13 | CB | H-accepter | 3.36 | -0.1 | PHE300 | |
| 8 | N5 | OD1 | H-donor | 3.19 | -1.4 | ASN347 | -9.1643 |
| | O4 | ND2 | H-accepter | 2.55 | -2.5 | ASN347 | |
| 9 | C6 | OD1 | H-donor | 3.25 | -0.3 | ASN347 | -10.6506 |
| | O4 | NE2 | H-accepter | 3.31 | -2.6 | HIS348 | |
| | O14 | OH | H-accepter | 3.23 | -1.6 | TYR344 | |
| | 6-ring | CE1 | π -H | 3.85 | -0.3 | PHE158 | |
| 10 | 5-ring | CD | π -H | 3.75 | -0.6 | ARG312 | -8.2309 |
| 11 | O4 | ND2 | H-accepter | 2.52 | -2.8 | ASN347 | -8.9435 |
| 12 | N5 | ODI | H-donor | 3.25 | -1.1 | ASN347 | -11.5231 |
| | C15 | ODI | H-donor | 3.31 | -0.0 | ASN347 | |
| | O4 | NH2 | H-accepter | 3.23 | -2.1 | ARG212 | |
| | O4 | CZ | H-accepter | 3.85 | -0.1 | PHE300 | |
| 13 | N1 | O | H-donor | 2.73 | -10.9 | ASP408 | -9.9815 |
| | C15 | OD2 | H-donor | 3.11 | -0.1 | PHE157 | |
| | C16 | OD2 | H-accepter | 3.34 | -0.1 | ARG312 | |
| | C21 | O | H-accepter | 2.74 | -4.2 | ARG312 | |
| 14 | O14 | CE1 | H-accepter | 2.72 | -0.6 | HIS111 | -9.5983 |
| | 5-ring | 6-ring | π - π | 3.84 | -0.0 | PHE177 | |
| 15 | N1 | O | H-donor | 3.40 | -0.2 | ASP349 | -10.9647 |
| | N5 | O | H-donor | 3.23 | -1.4 | ASP349 | |
| | C17 | OE1 | H-donor | 3.95 | -0.1 | GLN350 | |
| | O7 | CZ | H-accepter | 3.99 | -0.1 | PHE158 | |
| 16 | O4 | NE2 | H-accepter | 3.60 | -1.0 | HIS348 | -9.1089 |
| | 5-ring | 6-ring | π - π | 4.00 | -0.0 | PHE300 | |

(continued on next page)

Table 2 (continued)

| C. No. | Interaction details | | | | | | Docking score (S) |
|--------|---------------------|----------|---------------|----------|-----------|---------|-------------------|
| | Ligands | Receptor | | Distance | E cal/mol | residue | |
| 17 | 5-ring | 6-ring | π - π | 3.93 | -0.0 | PHE177 | -8.8934 |
| 18 | C6 | OE1 | H-donor | 3.06 | -2.2 | GLU276 | -9.0012 |
| | 5-ring | ND2 | π -H | 4.90 | -0.5 | ASN347 | |
| 19 | N1 | O | H-donor | 3.70 | -3.3 | PHE157 | -12.0905 |
| | N1 | CD1 | H-acceptor | 3.81 | -0.1 | PHE157 | |
| | O14 | CD2 | H-acceptor | 3.23 | -0.1 | LEU218 | |
| | O4 | N | H-acceptor | 1.9 | -4.4 | ARG312 | |
| | C22 | OD1 | H-donor | 3.0 | -0.1 | ASN347 | |
| | C21 | O | H-donor | 3.6 | -0.1 | ASP349 | |
| | C15 | 6-ring | H- π | 4.41 | -0.1 | TYR313 | |
| | C20 | 6-ring | H- π | 4.42 | -0.2 | PHE300 | |
| | C22 | 6-ring | H- π | 3.98 | -0.7 | PHE300 | |
| | 5-ring | CD2 | π -H | 4.38 | -0.1 | PHE300 | |
| 20 | O31 | OH | H-acceptor | 2.87 | -0.6 | TYR344 | -9.1220 |
| | 5-ring | 6-ring | π - π | 2.86 | -0.0 | PHE300 | |

alkyl substitutions. Among both the categories, we have noticed several potent compounds compared among the categories. Also, we have observed that changing the position of the substituted group ultimately affects the enzymatic activity. The magnitude of activation of the alkyl group is more moderate than the compounds that hold the deactivated group, even though they are di-substituted, i.e., compound **5–7**, and **8** which holds two deactivated groups at different positions of the benzene ring. The magnitude of deactivation of these halogen groups is much weaker than the alkyl group, which could donate most of their electronic density to the π -system, while the deactivation groups, which could withdraw most of the electronic density from the π -system, resulting in the partial positive charge on the ring, and hence remain unstable and this way the enzymatic activity remains less than the compound that holds the activated group and resulting donating electronic density, hence the access of the π -system are richer and enhance the enzymatic activity overall. Figure-11 (Supp. inf.) displays the mode of interaction of the most active compounds.

We also noticed that the compounds substituted with the alkyl groups showed less activity on a gradual pattern, i.e., compounds **13–14**, **16–18**, and **20**, while compound **19** which has 9 carbon showed the highest potential. These results delineate that the compound holding the alkyl group by the pattern ($= >6 < 9$) showed the highest potential than other compounds. The increase in the carbon quantity does matter, due to the active site of the enzyme, which couldn't accommodate this high-profile compound, i.e., compound **20** (20 carbons). The highest potential of ranked first compound might be due to the well-accommodated pattern of binding in the active site of the enzyme. In general, the molecular docking results explain that the compounds that hold the donating groups showed the best potential than the compounds that hold withdrawing groups. Also, we have noticed that compounds that hold longer carbon chain at their substituted position (compound **20**) were not well accommodated in the

active site, resulting in less activity than the compound that holds a similar group i.e., alkyl but with less no. of carbons (compound **19**).

2.8. Inspecting the stability of α -glucosidase in presence of potent compound

Molecular docking results revealed a fit-well binding pattern of compound **19** with the adaptation of several key interactions with active site residues. Furthermore, we have performed molecular dynamics (MD) simulation, to show the stability of the overall complex (α -glucosidase + c19) in an explicit watery environment. Generally, it was observed that the compound showed an inverted V-like illustration in the active site of the enzyme, where one end of the compound (the alkyl group) of the compound remains stick with the key residues and the other side stick with other residues and the overall active site of the compound represent a cave-like structure. For the ease of clarification and support of dynamics results, we further analyzed the dynamics trajectory.

The deviation of backbone atoms was examined by root-mean-square-deviation (RMSD). The RMSD of the system relative to the original structures illustrates that 50 ns simulation time is adequate to attain equilibration at temperature 310 K (Fig. 12A). The low RMSD curve supports the high stability of the conformation and vice versa. Initially, the RMSD curve gradually goes upward and oscillates after 37 ns simulation time, hence we have extracted that conformation, and were compared it with the rest of the conformations extracted from the later simulation time. Interestingly, we have found both the conformations the same, but solely found differences in the 6-AF conformation, where the alkyl group over the benzene ring rotates by 10°. The RMSD curve indicates the stabilized behaviors of the overall complex, wherein most of the simulation time the c19 resides tightly with the bonded residues in the active site. This tight binding to the active site indicates a crucial role of c19 in protein stability, which rescues the

protein from activation. To clarify further the specificity of this compound bonding in the active site dynamically. We have analyzed the root-mean-square-fluctuation (RMSF). The results indicate a high fluctuation in the active site where this compound bonded with several key residues, and some local fluctuation was observed in the terminal region of the enzyme, where a bunch of single loops fluctuated most of the simulation time (Fig. 12B). These results delineate that this compound binding stabilized the overall conformation of the protein and might rescue them from activation.

2.9. Cytotoxicity and carcinogenicity prediction

All the twenty compounds were predicted as non-cytotoxic and the probability of the cytotoxicity is described in Table 3. Furthermore, the carcinogenicity was also evaluated by the ProtoxII server. Out of 20 compounds, a total of seven compounds **1**, **3**, **4**, **9**, **10**, **11**, and **12** were predicted as carcinogenic with the probability scores of carcinogenicity 0.88, 0.65, 0.65, 0.69, 0.89, 0.89, and 0.62, respectively. All the remaining compounds were predicted as non-carcinogenic.

2.10. Conclusion

In conclusion, twenty (**1–20**) different nitrofurazone derivatives were synthesized by using alkyl/benzyl halides. Out of twenty derivatives, fourteen were new, while six have been reported previously. All synthetic compounds showed higher α -glucosidase inhibition than nitrofurazone. The synthetic molecules were divided into two categories based on their substitution, among benzyl derivatives, the chloro substituted derivatives **2**, **4**, **6**, and **7** showed potential inhibition against the α -glucosidase enzyme, which might be associated with the position and number of chloro groups helping these molecules to attain the best position to fit in the active pocket of the enzyme. Nevertheless, the alkyl-substituted compounds **15** and

19 also displayed good α -glucosidase inhibition, and compound **19** was the most active compound of the series. The binding conformation of most active compounds was determined by a molecular docking study. The docking studies revealed that structural features of active compounds play a vital role in the binding interactions of compounds with the enzyme. The kinetic studies of most active compounds **7** and **19** showed that these compounds exhibit a competitive and uncompetitive mode of inhibition, respectively. The synthetic molecules were also examined for cytotoxicity and carcinogenicity. All the compounds were predicted as non-cytotoxic, however, few compounds **1**, **3**, **4**, **9**, **10**, **11**, and **12** were predicted as carcinogenic. The current study has identified new and potential α -glucosidase inhibitors which may act as lead compounds for drug discovery and research. However, further studies must be carried out to evaluate their cytotoxic effect thus confirming them as potential lead molecules or drug candidates.

3. Experimental

3.1. Materials and method

Dried glasswares were used for all the reactions, chemical reagents were purchased either from E-Merck or Sigma-Aldrich (USA). Evaporation of organic solvent was carried out by rotatory evaporator (Büchi rotavapor 210) with a water bath temperature of 35 °C. Nitrofurazone was provided by Nabi Qasim Pharmaceutical Industries Pvt. TLC (thin layer chromatography) was performed on Merck Kieselgel 60 F₂₅₄ silica gel sheets. Visualizations of spots were carried out with UV light (254 and 366 nm) and iodine vapors. Melting points (m.p.) were measured by Büchi melting point M.560 apparatus in open glass capillary tubes and are uncorrected. EI-MS and HR-EIMS spectra were recorded on JEOL JMS 600H-1 and JEOL JMS-HX-110, respectively. Bruker Avance spectropho-

Table 3 Prediction of carcinogenicity and cytotoxicity of the compounds.

| C. No. | Carcinogenicity | Cytotoxicity | Probability of carcinogenicity | Probability of cytotoxicity |
|-----------|-----------------|--------------|--------------------------------|-----------------------------|
| 1 | Active | Inactive | 0.88 | 0.91 |
| 2 | Inactive | Inactive | 0.50 | 0.85 |
| 3 | Active | Inactive | 0.65 | 0.86 |
| 4 | Active | Inactive | 0.65 | 0.86 |
| 5 | Inactive | Inactive | 0.50 | 0.85 |
| 6 | Inactive | Inactive | 0.50 | 0.85 |
| 7 | Inactive | Inactive | 0.50 | 0.85 |
| 8 | Inactive | Inactive | 0.56 | 0.83 |
| 9 | Active | Inactive | 0.69 | 0.60 |
| 10 | Active | Inactive | 0.89 | 0.91 |
| 11 | Active | Inactive | 0.89 | 0.91 |
| 12 | Active | Inactive | 0.62 | 0.89 |
| 13 | Inactive | Inactive | 0.55 | 0.79 |
| 14 | Inactive | Inactive | 0.54 | 0.81 |
| 15 | Inactive | Inactive | 0.65 | 0.81 |
| 16 | Inactive | Inactive | 0.52 | 0.8 |
| 17 | Inactive | Inactive | 0.58 | 0.78 |
| 18 | Inactive | Inactive | 0.58 | 0.78 |
| 19 | Inactive | Inactive | 0.58 | 0.78 |
| 20 | Inactive | Inactive | 0.58 | 0.78 |

tometer 400/100 MHz was used for ^1H NMR and ^{13}C NMR, respectively. Chemical shifts (δ) are in ppm and coupling constants (J) are in Hz.

3.2. General synthetic procedure for compounds 1–20

In a 100 mL round-bottomed flask, nitrofurazone (2 mmol) was dissolved in DMF (10 mL), K_2CO_3 (1.2 equivalent) was also added and the reaction mixture was stirred for 10 min, then alkyl/ substituted benzyl halides (2 mmol) were added and it was refluxed for 6–12 h. The reaction progress was monitored through TLC (Hex: EtOAc, 1:1). When the reaction was completed, the reaction mixture was filtered to separate K_2CO_3 and the filtrate was poured into distilled water. The product was extracted by using dichloromethane. Anhydrous sodium sulfate (Na_2SO_4) was used to remove water molecules from organic, further, it was evaporated *in vacuo* and washed with ethyl acetate to afford the pure product (**1–20**) (Khan et al., 2018).

3.3. α -Glucosidase inhibition assay

α -Glucosidase inhibition assay was performed following the literature procedure (Solangi et al., 2020) Briefly, the solutions of α -glucosidase (*Saccharomyces cerevisiae* 2.5 U MI-1 purchased from Sigma-Aldrich, USA) and the substrate, *p*-nitrophenyl α -D-glucopyranoside (*p*-NPG) were prepared in 0.07 M phosphate buffer (pH 6.8). The buffer (70 μL) was pre-incubated along with 10 μL of the enzyme and 10 μL of the test compound at 37 $^\circ\text{C}$ for 5 min. The 96 well plates were further incubated for 30 min at the same temperature after the addition of 10 μL of *p*-NPG (10 mM) to each well. 80 μL Na_2CO_3 solution (0.2 M) was added to quench the reaction. The test compounds were not added in negative control wells, however, 10 μL of buffer was additionally added to them. Acarbose was used as the positive control. The absorbance was measured at a wavelength of 405 nm using a microplate reader (Bio-Tek ELx 800TM, Winooski, USA) which determined the activity of test compounds against α -glucosidase. The following formula was used for the calculation of percent inhibition.

Percent inhibition (%)

$$= [1 (\text{Absorbance of sample} / \text{Absorbance of control}) 100]$$

Dose-response curves of potential inhibitors ($\geq 50\%$) were obtained and IC_{50} was determined with the help of the GraphPad Prism 5.0 Software Inc., San Diego, California, USA.

3.4. Molecular docking (MD) protocol

Molecular docking studies were carried out to explore the inhibition mechanism of nitrofurazone derivatives against the α -glucosidase enzyme. The α -glucosidase model used in this study was previously reported by our group (Chemical Computing Group (CCG) Inc. Molecular Operating Environment (MOE); Chemical Computing Group: Montreal, QC, Canada, 2019). The chemical structure of nitrofurazone derivatives was built by Molecular Operating Environment (MOE) version 2019.0137 builder module and minimized by MMFF94x forcefield. MOE-dock Program was used to explore the binding modes of each molecule.

The stability of molecules was ensured by analyzing hydrogen bonding and hydrophobic interactions of molecules with the respective target through MOE-Protein Ligand Interaction Fingerprint (PLIF) Program.

3.5. Molecular dynamic simulation

First, the generalized Amber force field (GAFF) (Wang et al., 2004) was used to parameterize c19. Single-point energy calculations utilizing Schrodinger's quantum chemistry module, Jaguar, employing the Hartree-Fock level of theory and the 6-311 g** basis set established the partial atomic charges. The Antechamber module (Wang et al., 2006) was used to assign the GAFF atom types, and the AMBER LEaP module was used to generate the parameter file (Delano, 2010). AMBER version 2018 (Case et al., 2018) was used to perform all-atom MD simulations and essential dynamics analyses. Hydrogen atoms were included in the homology model of the enzyme using the LEaP module. Counter ions were then introduced to keep the system neutral. The system was solvated in the TIP3P water model truncated octahedral box with a cut-off of 10.0 \AA buffer. All MD simulations were accelerated using the CUDA version of PMEMD. The detail molecular dynamics simulation methodology has been described in detail in our previous study (Rehman et al., 2020; Rehman et al., 2019; Rehman et al., 2019; Rehman et al., 2021).

3.6. Kinetics of α -glucosidase inhibition

To find out inhibition mode (competitive, uncompetitive, non-competitive, or mixed) of the most potent compounds against α -glucosidase, the enzyme kinetics study was performed according to the described protocol by Elahabaadi et al. with slight modification (Elahabaadi et al., 2021). Compounds **7** and **19** having IC_{50} 0.65 ± 0.22 and 0.54 ± 0.30 μM , respectively, were selected for this study. These compounds were tested with concentrations of 0, 0.3, 0.6, and 0.9 μM against enzyme at various concentrations of *p*-nitrophenyl α -D-glucopyranoside (4–20 mM). The reaction mixture was incubated at 37 $^\circ\text{C}$ for 30 min and the reading was taken at a wavelength of 405 nm using a microplate reader (Bio-Tek ELx 800TM, Winooski, USA). Lineweaver–Burk's plots were obtained with the help of GraphPad prism 5.0 Software Inc., San Diego, California, USA.

3.7. Carcinogenicity and cytotoxicity prediction

Carcinogens are chemicals that can cause tumors or develop the occurrence of tumors (Zhang et al., 2014). The ability to predict cytotoxicity is critical for screening chemical compounds that might cause the undesired as well as the desired cell harm, the latter being particularly relevant in the case of tumor cells (Banerjee et al., 2018). The ProTox-II online server was used to predict the carcinogenicity of the compounds. The ProTox-II is a simple and self-explanatory user interface server. The name of the compound or the SMILES string of the compound is required as input to estimate the probable toxicities of the compound. The chemical editor (<https://www.chemdoodle.com/>) also allows the user to draw the structure of the compounds. The ProTox-II server was used

to predict the carcinogenicity and cytotoxicity of each compound (Kroes et al., 2004).

3.8. *N*-(Benzyl)-2-((5-nitrofurazan-4-yl)methylene)hydrazine Carboxamide (1)

Compound **1** was obtained as yellow amorphous powder with 66% yield. R_f value = 0.46 (Hex:EtOAc, 1:1); Melting point; 167–168 °C; ^1H NMR: (400 MHz, DMSO d_6): δ_H 7.74 (d, 1H, $J_{2,3} = 4.0$ Hz, H-2), 7.52 (s, 1H, H-5), 7.40 (d, 1H, $J_{3,2} = 4.0$ Hz, H-3), 7.36 (d, 2H, $J_{3',6'} = 7.2$ Hz, H-2', H-6'), 7.26 (m, 4H, H-3', H-4', H-5', NH-1), 3.16 (s, 1H, NH-2), 5.18 (s, 2H, CH₂). EI-MS: m/z (rel. abund. %) 288 (M^+ , 18), 245 (56), 202 (20), 154 (33), 149 (85), 106 (43), 91 (100), 79 (23), 51 (12). HREI-MS: m/z Calcd. for C₁₃H₁₂N₄O₄ 288.0859, Found 288.0849.

3.9. *N*-(2'-Chlorobenzyl)-2-((5-nitrofurazan-2-yl) methylene) hydrazinecarboxamide (2)

Compound **2** was obtained as pale-yellow amorphous powder with 62% yield. R_f value = 0.34 (Hex:EtOAc, 1:1); Melting point; 198–199 °C; ^1H NMR: (400 MHz, MeOD- d): δ_H 7.80 (s, 1H, H-5), 7.51 (d, 1H, $J_{2,3} = 4.0$ Hz, H-2), 7.39 (t, 1H, $J_{5',6'} = 7.7$ Hz, H-5'), 7.29 (d, 1H, $J_{3',6'} = 1.6$ Hz, H-3'), 7.26 (t, 1H, $J_{4'(3'5')} = 1.6$ Hz, H-4'), 7.24 (d, 1H, $J_{6',3'} = 1.6$ Hz, H-6'), 7.04 (d, 1H, $J_{3,2} = 4.0$ Hz, H-3), 4.56 (s, 2H, CH₂). ^{13}C NMR: (75 MHz, DMSO d_6): δ_C 154.9 (C = O), 152.8 (C-1), 151.3 (C-4), 137.0 (C-1'), 131.5 (C-3'), 129.0 (C-6'), 128.3 (C-2'), 128.1 (C-5'), 127.1 (C-5), 115.1 (C-2), 112.0 (C-3), 40.46 (CH₂). EI-MS: m/z (rel. abund. %) 323 (M^+ , 1), 305 (9), 287 (98), 276 (2), 255 (3), 181 (5), 167 (8), 155 (100), 140 (25), 132 (26), 125 (89), 106 (29), 89 (19), 79 (23), 51 (20). HREI-MS: m/z Calcd. for C₁₃H₁₁ClN₄O₄ 322.0469, Found 322.0455.

3.10. *N*-(3'-Chlorobenzyl)-2-((5-nitrofurazan-2-yl) methylene) hydrazinecarboxamide (3)

Compound **3** was obtained as pale-yellow amorphous powder with 64% yield. R_f value = 0.47 (Hex:EtOAc, 1:1); Melting point; 229–230 °C; ^1H NMR:(400 MHz, MeOD- d): δ_H (s, 1H, H-5), 7.51 (d, 1H, $J_{2,3} = 4.0$ Hz, H-2), 7.34 (s, 1H, NH-1), 7.29 (s, 1H, H-2'), 7.27 (d, 1H, $J_{4',5'} = 5.2$ Hz, H-4'), 7.24 (d, 1H, $J_{6',4'} = 2.0$ Hz, H-6'), 7.22 (d, 1H, $J_{5',4'} = 7.6$ Hz, H-5'), 4.44 (s, 2H, CH₂). ^{13}C NMR: (75 MHz, DMSO d_6): δ_C 154.9 (C = O), 152.8 (C-1), 143.0 (C-1'), 132.8 (C-3'), 130.1 (C-5), 127.9 (C-2'), 126.8 (C-6'), 126.5 (C-4'), 125.7 (C-5'), 115.1 (C-2), 112.6 (C-3), 42.0 (s, 2H, CH₂). EI-MS: m/z (rel. abund. %) 322 (M^+ , 9), 183 (3), 169 (93), 155 (100), 140 (34), 132 (70), 125 (81), 111 (9), 106 (30), 96 (4), 89 (13), 77 (15), 51 (10). HR-EIMS: m/z Calcd. for C₁₃H₁₁ClN₄O₄ 322.0469, Found 322.0467.

3.11. *N*-(4'-Chlorobenzyl)-2-((5-nitrofurazan-2-yl)methylene) hydrazine Carboxamide (4)

Compound **4** was obtained as pale-yellow amorphous powder with 66% yield. R_f value = 0.46 (Hex:EtOAc, 1:1); Melting point; 269–270 °C; ^1H NMR: (400 MHz, MeOD- d): δ_H 7.86

(s, 1H, NH-1), 7.50 (s, 1H, H-5), 7.48 (d, 2H, $J_{2',6'} = 3',5' = 8.4$ Hz, H-3', H-5'), 7.46 (d, 1H, $J_{2,3} = 3.6$ Hz, H-2), 7.17 (d, 2H, $J_{2',6'} = 3',5' = 8.4$ Hz, H-2', H-6'), 7.01 (d, 1H, $J_{3,2} = 4.0$ Hz, H-3), 5.19 (s, 1H, NH-2), 4.55 (s, 2H, CH₂). ^{13}C NMR: (75 MHz, DMSO d_6): δ_C 154.9 (C = O), 152.9 (C-1), 151.3 (C-4), 139.4 (C-1'), 131.1 (C-4'), 128.9 (C-3', C-5'), 128.1 (C-2', C-6'), 127.8 (C-5), 115.1 (C-2), 112.5 (C-3), 41.9 (CH₂). EI-MS: m/z (rel. abund. %) 322 (M^+ , 5), 305 (34), 181 (4), 166 (20), 155 (77), 140 (8), 79 (8), 51 (8), 44 (9). HREI-MS: m/z Calcd. for C₁₃H₁₁ClN₄O₄ 322.0469, Found 322.0466.

3.12. *N*-(2',4'-Dichlorobenzyl)-2-((5-nitrofurazan-2-yl) methylene)hydrazine carboxamide (5)

Compound **5** was obtained as pale-yellow amorphous powder with 72% yield. R_f value = 0.44 (Hex:EtOAc, 1:1); Melting point; 236–237 °C; ^1H NMR: (400 MHz, DMSO d_6): δ_H 7.80 (s, 1H, H-5), 7.76 (d, 1H, $J_{3',5'} = 4.0$ Hz, H-3'), 7.69 (d, 1H, $J_{5',3'} = 2.0$ Hz, H-5'), 7.43 (d, 2H, $J_{6',5'} = 5.0$ Hz, H-6'), 7.21 (s, 2H, NH-1, NH-2), 6.81(d, 1H, $J_{3,2} = 8.4$ Hz, H-3), 5.15 (s, 2H, CH₂). ^{13}C NMR: (75 MHz, DMSO d_6): δ_C 154.9 (C = O), 152.7 (C-1), 136.4 (C-4), 132.4 (C-4), 132.4 (C-1'), 131.9 (C-2'), 129.5 (C-4), 128.4 (C-3'), 128.2 (C-5'), 127.7 (C-6'), 127.3 (C-5), 115.1 (C-2), 112.8 (C-3), 40.1 (CH₂). EI-MS: m/z (rel. abund. %) 357 (M^+ , 1), 341 (16), 321 (32), 201 (25), 159 (100), 155 (94), 140 (63), 79 (35), 51 (41), 43 (8). HR-EIMS: m/z Calcd. for C₁₃H₁₀Cl₂N₄O₄ 356.0079, Found 356.0098.

3.13. *N*-(2',6'-Dichlorobenzyl)-2-((5-nitrofurazan-2-yl) methylene)hydrazine Carboxamide (6)

Compound **6** was obtained as yellow amorphous powder with 61% yield. R_f value = 0.45 (Hex:EtOAc, 1:1); Melting point; 240–241 °C; ^1H NMR: (400 MHz, MeOD- d): δ_H 7.80(s, 1H, H-5), 7.51 (d, 1H, $J_{2,3} = 4.0$ Hz, H-2), 7.39 (t, 2H, $J_{4'(3'5')} = 7.2$ Hz, H-4', NH-1), 7.28 (m, 2H, H-3', H-5'), 7.04 (d, 1H, $J_{3,2} = 4.0$ Hz, H-3), 5.46 (s, 1H, NH-2), 4.56 (s, 2H, CH₂). ^{13}C NMR: (75 MHz, DMSO d_6): δ_C 154.0 (C = O), 152.5 (C-1), 151.3 (C-4), 135.3 (C-1'), 133.8 (C-2'), 130.1 (C-5), 128.7 (C-3', C-5'), 128.1 (C-4'), 115.0 (C-2), 113.0 (C-3), 39.40 (CH₂). EI-MS: m/z (rel. abund. %) 357 (M^+ , 1), 341 (2), 321 (32), 201 (25), 174 (26), 166 (71), 159 (100), 155 (94), 140 (63), 123 (22), 111 (19), 79 (35), 70 (19), 51 (1), 43 (8). HREI-MS: m/z Calcd. for C₁₃H₁₀Cl₂N₄O₄ 356.0079, Found 356.00160.

3.14. (3',4'-Dichlorobenzyl)-2-((5-nitrofurazan-2-yl)methylene) hydrazine carboxamide (7)

Compound **7** was obtained as yellow amorphous powder with 69% yield. R_f value = 0.46 (Hex:EtOAc, 1:1); Melting point; 236–237 °C; ^1H NMR: (400 MHz, MeOD- d): δ_H 8.30 (s, 1H, H-3'), 7.54 (s, 1H, H-5), 7.43 (dd, 3H, $J_{3',5'} = 8.8$ Hz, H-3', H-5', NH-1), 7.34 (d, 1H, $J_{2,3} = 3.6$ Hz, H-2), 7.19 (dd, 1H, $J_{2',6'} = 8.4$ Hz, H-6'), 6.79 (d, 1H, $J_{3,2} = 4.0$ Hz, H-3), 5.27 (s, 1H, NH-2), 4.50 (s, 2H, CH₂). ^{13}C NMR: (75 MHz, DMSO d_6): δ_C 154.9 (C = O), 152.7 (C-1), 141.7 (C-1'), 130.4 (C-5), 129.0 (C-3'), 129.0 (C-4'), 128.08 (C-2', C-5'), 127.4 (C-6'), 115.1 (C-2), 112.7 (C-3), 41.6 (CH₂). EI-MS:

m/z (rel. abund. %) 357 (M^+ , 1), 339 (4), 201 (34), 174 (25), 166 (100), 159 (76), 140 (27), 123 (24), 109 (11), 89 (10), 75 (14), 51 (14), 44 (7), HREI-MS: m/z Calcd. for $C_{13}H_{10}Cl_2N_4O_4$ 356.0079, Found 356.0098.

3.15. *N*-(2'-Chloro-4'-fluorobenzyl)-2-((5-nitrofur-2-yl)methylene) hydrazine carboxamide (8)

Compound **8** was obtained as brown amorphous powder with 77% yield. R_f value = 0.46 (Hex:EtOAc, 1:1); Melting point; 198–199 °C; 1H NMR: (400 MHz, $CDCl_3$ -*d*): δ_H 7.31 (d, 1H, $J_{2,3} = 3.6$ Hz, H-5), 7.18 (dd, 1H, $J_{3',5'} = 2.4$ Hz, $J_{5',6'} = 8.4$ Hz, H-5'), 7.11 (s, 1H, H-5), 6.98 (dd, 1H, $J_{6',3'} = 2.4$ Hz, $J_{6',5'} = 8.4$ Hz, H-6'), 6.95 (dd, 1H, $J_{3',5'} = 2.4$ Hz, $J_{3',6'} = 7.6$ Hz, H-3'), 6.72 (d, 1H, $J_{3,2} = 4.0$ Hz, H-3), 4.55 (s, 2H, CH_2). ^{13}C NMR: (75 MHz, DMSO d_6): δ_C 163.6 (C-4'), 160.2 (C=O), 155.9 (C-1), 151.7 (C-4), 149.6 (C-1'), 133.1 (C-2'), 128.4 (C-6'), 125.4 (C-5), 117.6 (C-3'), 115.0 (C-5'), 14.7 (C-2), 113.1 (C-3), 42.3 (CH_2). EI-MS: m/z (rel. abund. %) 340 (M^+ , 30), 305 (26), 297 (80), 254 (26), 201 (52), 167 (28), 158 (33), 143 (100). HREI-MS: m/z Calcd. for $C_{13}H_{10}ClFN_4O_4$ 340.0375, Found 340.03806.

3.16. *N*-(4'-Bromobenzyl)-2-((5-nitrofur-2-yl)methylene) hydrazine Carboxamide (9)

Compound **9** was obtained as brown amorphous powder with 63% yield. R_f value = 0.47 (Hex:EtOAc, 1:1); Melting point; 235–236 °C; 1H NMR: (400 MHz, MeOD-*d*): δ_H 7.50 (d, 2H, $J_{2,6'} = 3',5' = 8.4$ Hz, H-3', H-5'), 7.48 (s, 1H, NH-1), 7.46 (d, 1H, $J_{2,3} = 3.6$ Hz, H-2), 7.17 (d, 2H, $J_{3',5'} = 2',6' = 8.4$ Hz, H-2', H-6'), 7.01 (d, 1H, $J_{3,2} = 4.0$ Hz, H-3), 5.19 (s, 1H, NH-2), 4.55 (s, 2H, CH_2). ^{13}C NMR: (75 MHz, DMSO d_6): δ_C 155.8 (C = O), 153.4 (C-1), 151.4 (C-4), 134.8 (C-1'), 131.5 (C-3', C-5'), 128.9 (C-2', C-6'), 125.2 (C-4'), 120.2 (C-5), 115.2 (C-2), 111.2 (C-3), 43.1 (CH_2). EI-MS: m/z (rel. abund. %) 368 (M^+ , 4), 323 (11), 291 (2), 282 (7), 229 (53), 184 (27), 169 (100), 154 (10), 132 (4), 90 (23), 79 (8), 63 (4), 51 (7), 44 (2). HREI-MS: m/z Calcd. for $C_{13}H_{11}BrN_4O_4$ 365.9964, Found 365.9971.

3.17. *N*-(3-Methylbenzyl)-2-((5-nitrofur-2-yl)methylene) hydrazine Carboxamide (10)

Compound **10** was obtained as yellow amorphous powder with 71% yield. R_f value = 0.47 (Hex:EtOAc, 1:1); Melting point ; 189–190 °C; 1H NMR: (400 MHz, DMSO d_6): δ_H 7.74 (d, 1H, $J_{2,3} = 4.0$ Hz, H-2), 7.49 (s, 1H, H-5), 7.40 (d, 1H, $J_{3,2} = 4.0$ Hz, H-3), 7.22 (t, 2H, $J_{5'(4'/6')} = 7.6$ Hz, H-5', NH-1), 7.06 (d, 1H, $J_{2',4'} = 7.6$ Hz, H-2'), 7.01 (d, 2H, $J_{4',6'} = 11.2$, H-4', H-6'), 6.51 (s, 1H, NH-2), 5.14 (s, 2H, CH_2), 2.26 (s, 3H, aromatic CH_3). ^{13}C NMR: (75 MHz, DMSO d_6): δ_C 156.2 (C = O), 153.8 (C-1), 138.2 (C-4), 135.5 (C-1'), 128.9 (C-3'), 128.2 (C-2'), 127.3 (C-5'), 125.3 (C-4'), 123.9 (C-5) 115.6 (C-2), 111.6 (C-3), 44.0 (CH_2), 21.3 (aromatic CH_3). EI-MS: m/z (rel. abund. %) 302 (M^+ , 2), 259 (32), 240 (2), 225 (4), 200 (3), 163 (17), 138 (3), 120 (13), 57 (6), 43 (12). HREI-MS: m/z Calcd. for $C_{14}H_{14}N_4O_4$ 302.1015, Found 302.1006.

3.18. *N*-(4-Methylbenzyl)-2-((5-nitrofur-2-yl)methylene) hydrazine carboxamide (11)

Compound **11** was obtained as yellow amorphous powder with 86% yield. R_f value = 0.47 (Hex:EtOAc, 1:1); Melting point; 185–186 °C; 1H NMR: (500 MHz, MeOD-*d*): δ_H 8.54 (s, 1H, H-5), 7.44 (d, 1H, $J_{2,3} = 4.0$ Hz, H-2), 7.22 (d, 2H, $J_{2',6'} = 3',5' = 8.4$ Hz, H-2', H-6'), 7.48 (s, 1H, NH-1), 7.17 (d, 2H, $J_{3',5'} = 2',6' = 8.4$ Hz, H-3', H-5'), 6.22 (d, 1H, $J_{3,2} = 4.0$ Hz, H-3), 5.19 (s, 1H, NH-2), 4.41 (s, 2H, CH_2), 2.31 (s, 3H, aromatic CH_3). ^{13}C NMR: (75 MHz, DMSO d_6): δ_C 158.5 (C = O), 154.0 (C-1), 151.3 (C-4), 135.4 (C-1'), 129.0 (C-3', C-5'), 127.7 (C-2', C-6'), 127.8 (C-5), 125.1 (C-4'), 118.3 (C-2), 116.3 (C-3), 50.4 (CH_2), 20.6 (aromatic CH_3). EI-MS: m/z (rel. abund. %) 302.2 (M^+ , 2), 259 (32), 240 (2), 225 (4), 200 (3), 163 (17), 138 (3), 120 (13), 57 (6), 43 (12). HREI-MS: m/z Calcd. for $C_{14}H_{14}N_4O_4$ 302.1015, Found 302.1008.

3.19. *N*-(3'-Methoxybenzyl)-2-((5-nitrofur-2-yl)methylene) hydrazine carboxamide (12)

Compound **12** was obtained as yellow amorphous powder with 74% yield. R_f value = 0.44 (Hex:EtOAc, 1:1); Melting point; 199–200 °C; 1H NMR: (400 MHz, MeOD-*d*): δ_H 7.80 (s, 1H, H-5), 7.75 (d, 1H, $J_{2,3} = 3,2 = 4.0$ Hz, H-2), 7.51 (s, 1H, H-2'), 7.40 (d, 1H, $J_{3,2} = 2,3 = 4.0$ Hz, H-3), 7.27 (t, $J_{5'(4'/6')} = 8.0$ Hz, H-5'), 7.11 (s, 1H, NH-1), 6.82 (s, 1H, NH-2), 6.80 (t, 1H, $J_{6'(5'/2')} = 8.0$ Hz, H-6'), 6.72 (d, 1H, $J_{4',5'} = 7.6$ Hz, H-4'), 5.14 (s, 2H, CH_2), 3.71 (s, 3H, aromatic OCH_3). ^{13}C NMR: (75 MHz, DMSO d_6): δ_C 159.5 (C=O), 155.9 (C-1), 153.4 (C-4), 136.9 (C-1'), 129.8 (C-5), 125.2 (C-5'), 118.5 (C-6'), 115.2 (C-2), 112.6 (C-4'), 112.3 (C-3), 111.4 (C-2'), 54.9 (aromatic OCH_3), 43.6 (CH_2). EI-MS: m/z (rel. abund. %) 318 (M^+ , 4), 275 (11), 179 (52), 154 (4), 136 (33), 121 (100), 91 (18), 77 (5), 51 (4). HREI-MS: m/z Calcd. for $C_{14}H_{14}N_4O_5$ 318.0964, Found 318.0955.

3.20. 2-((5-Nitrofur-2-yl)methylene)-*N*-ethyl hydrazine carboxamide (13)

Compound **13** was obtained as yellow amorphous powder with 69% yield. R_f value = 0.48 (Hex:EtOAc, 1:1); Melting point; 155–156 °C; 1H NMR: (400 MHz, $CDCl_3$ -*d*): δ_H 7.42 (s, 1H, H-5), 7.36 (d, 1H, $J_{2,3} = 4.0$ Hz, H-2), 6.77 (d, 1H, $J_{3,2} = 4.0$ Hz, H-3), 4.02 (q, 2H, $J = 7.2$ Hz, CH_2), 1.19 (t, 3H, $J = 6.8$ Hz, CH_3). EI-MS: m/z (rel. abund. %) 226 (M^+ , 30), 210 (2), 183 (92), 168 (100), 154 (35), 138 (6), 121 (30), 109 (15), 93 (26), 79 (71), 67 (13), 51 (50), 42 (15).

3.21. 2-((5-Nitrofur-2-yl)methylene)-*N*-propyl hydrazine carboxamide (14)

Compound **14** was obtained as yellow amorphous powder with 83% yield. R_f value = 0.47 (Hex:EtOAc, 1:1); Melting point; 184–185 °C; 1H NMR: (400 MHz, $CDCl_3$ -*d*): δ_H 7.39 (s, 1H, H-5), 7.36 (d, 1H, $J_{2,3} = 4.0$ Hz, H-2), 6.77 (d, 1H, $J_{3,2} = 4.0$ Hz, H-3), 3.91 (t, 2H, $J = 7.6$ Hz, H-1'a,b), 1.62 (m, 2H, H-2'a, b), 0.97 (t, 3H, $J = 7.3$ Hz, CH_3). EI-MS:

m/z (rel. abund. %) 240 (M^+ , 13), 197 (26), 168 (100), 154 (11), 128 (6), 121 (9), 93 (7), 79 (9), 63 (7), 51 (5), 43 (7), 4 (5).

3.22. 2-((5-Nitrofurazan-2-yl) methylene)-N-butyl hydrazine carboxamide (15)

Compound **15** was obtained as yellow amorphous powder with 79% yield. R_f value = 0.44 (Hex:EtOAc, 1:1); Melting point; 184–185 °C; 1H NMR: (400 MHz, $CDCl_3-d$): δ_H 7.39 (s, 1H, H-5), 7.36 (d, 1H, $J_{2,3}$ = 4.0 Hz, H-2), 6.77 (d, 1H, $J_{3,2}$ = 4.0 Hz, H-3), 3.91 (t, 2H, J = 7.6 Hz, H-1'a, b), 1.62 (m, 4H, H-2'a,b, H-3'a,b), 0.97 (t, 3H, J = 7.3 Hz, CH_3). EI-MS: m/z (rel. abund. %) 269 (M^+ , 13), 197 (26), 168 (100), 154 (11), 128 (6), 121 (9), 93 (7), 79 (9), 63 (7), 51 (5), 43 (7), 4 (5).

3.23. 2-((5-Nitrofurazan-2-yl)methylene)-N-but-3-enyl hydrazine carboxamide (16)

Compound **16** was obtained as yellow crystalline form with 83% yield. R_f value = 0.46 (Hex:EtOAc, 1:1); Melting point; 135–136 °C; 1H NMR: (400 MHz, $CDCl_3-d$): δ_H 7.41(s, 1H, H-5), 7.37 (d, 1H, $J_{2,3}$ = 4.0 Hz, H-2), 6.78 (d, 1H, $J_{3,2}$ = 4.0 Hz, H-3), 5.82 (m, 1H, H-3'), 5.13 (m, 2H, H-2'a,b), 4.02 (t, J = 7.2 Hz, H-1'a,b), 2.35 (dd, J = 7.2 Hz, 14.4 Hz, H4'a, b). ^{13}C NMR: (75 MHz, DMSO d_6): δ_C 155.5 (C = O), 154.2 (C-1), 151.4 (C-4), 135.0 (C-5), 124.6 (C-3'), 116.8 (C-1'), 115.4 (C-2), 111.2 (C-3), 39.4 (C-1'), 29.3 (C-4'). EI-MS: m/z (rel. abund. %) 252 (M^+ , 2), 208 (3), 206 (17), 168 (100), 149 (14), 121 (5), 93 (5), 55 (5). HREI-MS: m/z Calcd. for $C_{10}H_{12}N_4O_4$ 252.0859, Found 252.0861.

3.24. 2-((5-Nitrofurazan-2-yl)methylene)-N-pentyl hydrazine carboxamide (17)

Compound **17** was obtained as yellow amorphous powder with 81% yield. R_f value = 0.45 (Hex:EtOAc, 1:1); Melting point; 199–200 °C; 1H NMR: (400 MHz, $CDCl_3-d$): δ_H 7.39 (s, 1H, H-5), 7.37 (d, 1H, $J_{2,3}$ = 4.0 Hz, H-2), 6.77 (d, 1H, $J_{3,2}$ = 4.0 Hz, H-3), 3.93 (t, 2H, J = 7.6 Hz, H-1'a,b), 1.35 (m, 6H, H-2'a,b, H-3'a,b, H-4'a,b), 0.89 (t, 3H, J = 6.8 Hz, CH_3). ^{13}C NMR: (75 MHz, DMSO d_6): δ_C 155.6 (C = O), 154.3 (C-1), 151.0 (C-4), 124.3 (C-5), 115.5 (C-2), 111.1 (C-3), 40.0 (C-1'), 24.4 (C-3'), 21.9 (C-4'), 13.9 (C-5'). EI-MS: m/z (rel. abund. %) 268 (M^+ , 56), 251 (8), 225 (16), 208 (28), 191 (8), 182 (12), 168 (100), 154 (46), 141 (9), 121 (38), 93 (20), 79 (36), 70 (48), 51 (20). HR-EIMS: m/z Calcd. for $C_{11}H_{16}N_4O_4$ 268.1172, Found 268.11840.

3.25. 2-((5-Nitrofurazan-2-yl) methylene)-N-hexyl hydrazine carboxamide (18)

Compound **18** was obtained as yellow crystals with 79% yield. R_f value = 0.44 (Hex:EtOAc, 1:1); Melting point; 200–201 °C; 1H NMR: (400 MHz, $CDCl_3-d$): δ_H 7.39 (s, 1H, H-5), 7.37 (d, 1H, $J_{2,3}$ = 4.0 Hz, H-2), 6.77 (d, 1H, $J_{3,2}$ = 4.0 Hz, H-3), 3.93 (t, 2H, J = 7.6 Hz, H-1'a,b), 1.31 (m, 8H, H-2'a,b, H-3'a,b, H-4'a,b, H-5'a,b), 0.89 (t, 3H, J = 6.8 Hz, CH_3). EI-MS: m/z (rel. abund. %) 282 (3), 265 (4), 239 (36), 222 (14), 168 (100), 154 (25), 121 (42), 70 (39), 55 (20).

3.26. 2-((5-Nitrofurazan-2-yl) methylene)-N-octyl hydrazine carboxamide (19)

Compound **19** was obtained as yellow amorphous powder with 91% yield. R_f value = 0.47 (Hex:EtOAc, 1:1); Melting point; 66–67 °C; 1H NMR: (400 MHz, $CDCl_3-d$): δ_H 7.38 (s, 1H, H-5), 7.36 (d, 1H, $J_{2,3}$ = 4.0 Hz, H-2), 6.77 (d, 1H, $J_{3,2}$ = 4.0 Hz, H-3), 3.92 (t, 2H, J = 7.6 Hz, H-1'a,b), 1.31 (m, 12H, H-2'a,b, H-3'a,b, H-4'a,b, H-5'a,b, H-6'a,b), 0.87 (t, 3H, J = 6.8 Hz, CH_3). ^{13}C NMR: (75 MHz, DMSO d_6): δ_C 155.5 (C = O), 154.2 (C-1), 151.0 (C-4), 124.3 (C-5), 115.4 (C-2), 111.1 (C-3), 39.9 (C-1'), 24.4 (C-3'), 21.9 (C-4'), 13.9 (C-5'). EI-MS: m/z (rel. abund. %) 310 (M^+ , 19), 293 (9), 267 (56), 250 (23), 168 (100), 154 (31), 138 (26), 121 (58), 93 (30), 79 (35), 70 (58), 55 (21), 41 (37). HR-EIMS: m/z Calcd. for $C_{14}H_{22}N_4O_4$ 310.641, Found 310.6380.

3.27. 2-((5-Nitrofurazan-2-yl) methylene)-N-octadecyl hydrazine carboxamide (20)

Compound **20** was obtained as yellow amorphous powder with 85% yield. R_f value = 0.59 (Hex:EtOAc, 1:1); Melting point; 85–86 °C; 1H NMR: (400 MHz, $CDCl_3-d$): δ_H 7.38 (s, 1H, H-5), 7.36 (d, 1H, $J_{2,3}$ = 4.0 Hz, H-2), 6.77 (d, 1H, $J_{3,2}$ = 4.0 Hz, H-3), 3.93 (t, 2H, J = 7.6 Hz, H-1'a,b), 1.31 (m, 32H, H-2'a,b, H-3'a,b, H-4'a,b, H-5'a,b, H-6'a,b, H-7'a,b, H-8'a,b, H-9'a,b, H-10'a,b, H-11'a,b, H-12'a,b, H-13'a,b, H-14'a,b, H-15'a,b, H-16'a,b, H-17'a,b), 0.87 (t, 3H, J = 6.8 Hz, CH_3). ^{13}C NMR: (75 MHz, DMSO d_6): δ_C 156.0 (C = O), 154.2 (C-1), 151.3 (C-4), 124.8 (C-5), 115.6 (C-2), 111.7 (C-3), 48.8 (C-1'), 40.3 (C-2'), 31.5 (C-3'), 29.1 (C-4', C-5', C-6', C-7', C-8', C-9', C-10', C-11', C-12', C-13'), 28.9 (C-14'), 26.3 (C-15'), 24.89 (C-16), 22.3 (C-17'), 14.1 (CH_3). EI-MS: m/z (rel. abund. %) 450 (M^+ , 1), 407 (11), 362 (11), 335 (9), 266 (6), 240 (10), 181 (12), 168 (100), 123 (19), 70 (23), 55 (29), 43 (49). HR-EIMS: m/z Calcd. for $C_{24}H_{42}N_4O_4$ 450.3206, Found 450.32495.

Acknowledgement

We thankfully acknowledge the financial support of Sindh Higher Education Commission (SHEC), Pakistan *vide* letter No. NO.DD/SHEC/1-14/2014, Project code SHEC/SRSP/Med-3/15/2021-21.

Appendix A. Supplementary material

Supplementary data to this article can be found online at <https://doi.org/10.1016/j.arabjc.2022.103806>.

References

- Nashiru, O., Koh, S., Lee, S.Y., Lee, D.S., 2001. Novel α -glucosidase from extreme thermophile *Thermus caldophilus* GK24. BMB Reports 34 (4), 347–354.
- Park, H., Hwang, K.Y., Oh, K.H., Kim, Y.H., Lee, J.Y., Kim, K., 2008. Discovery of novel α -glucosidase inhibitors based on the virtual screening with the homology-modeled protein structure. Bioorg. Med. Chem. 16 (1), 284–292.
- Bosenberg, L.H., Van Zyl, D.G., 2008. The mechanism of action of oral antidiabetic drugs: a review of recent literature. J. Endocrinol. Metabol. Diabet. South Africa 13 (3), 80–88.

- Abbasi, M. A., Shah, S. A. H., Aziz-ur-Rehman, Siddiqui, S. Z., Hussain, G., Khan, K. M., Ashraf, M., Ejaz, S. A. (2017). Synthesis of (*E*)-*N*'-[1-(2,4-dihydroxyphenyl)ethylidene]substituted hydrazides as possible α -glucosidase and butyryl cholinesterase inhibitors, *Journal of the Chemical Society of Pakistan*, 39, 248-253.
- Davies, G., Henrissat, B., 1995. Structures and mechanisms of glycosyl hydrolases. *Structure* 3 (9), 853–859.
- Van de Laar, F.A., 2008. Alpha-glucosidase inhibitors in the early treatment of type 2 diabetes. *Vascular Health and Risk Management* 4 (6), 1189.
- Azam, S.S., Uddin, R., Wadood, A., 2012. Structure and dynamics of alpha-glucosidase through molecular dynamics simulation studies. *J. Mol. Liq.* 174, 58–62.
- Khan, K.M., Rahim, F., Wadood, A., Kosar, N., Taha, M., Lalani, S., Choudhary, M.I., 2014. Synthesis and molecular docking studies of potent α -glucosidase inhibitors based on biscoumarin skeleton. *Eur. J. Med. Chem.* 81, 245–252.
- Liu, Y., Zou, L., Ma, L., Chen, W.H., Wang, B., Xu, Z.L., 2006. Synthesis and pharmacological activities of xanthone derivatives as α -glucosidase inhibitors. *Bioorg. Med. Chem.* 14 (16), 5683–5690.
- de Melo, E.B., da Silveira Gomes, A., Carvalho, I., 2006. α - and β -Glucosidase inhibitors: chemical structure and biological activity. *Tetrahedron* 62 (44), 10277–10302.
- Fischer, P.B., Collin, M., Karlsson, G.B., James, W., Butters, T.D., Davis, S.J., Gordon, S., Dwek, R.A., Platt, F.M., 1995. The α -glucosidase inhibitor *N*-butyldeoxyojirimycin inhibits human immunodeficiency virus entry at the level of post-CD4 binding. *J. Virol.* 69 (9), 5791–5797.
- Yoshikawa, Y., Hirata, R., Yasui, H., Hattori, M., Sakurai, H., 2010. Inhibitory effect of CuSO₄ on α -glucosidase activity in ddY mice. *Metallomics* 2 (1), 67–73.
- Khan, M., Aftab, A., Khan, K.M., Salar, U., Chigurupati, S., Wadood, A., Ali, F., Mohammad, J.I., Riaz, M., Perveen, S., 2018. Flurbiprofen derivatives as novel α -amylase inhibitors: biology-oriented drug synthesis (BIODS), *in vitro*, and *in silico* evaluation. *Bioorg. Chem.* 81, 157–167.
- Mohiuddin, G., Khan, K.M., Salar, U., Lodhi, M.A., Wadood, A., Riaz, M., Perveen, S., 2019. Biology-oriented drug synthesis (BIODS), *in vitro* urease inhibitory activity, and *in silico* study of *S*-naproxen derivatives. *Bioorg. Chem.* 83, 29–46.
- Muhammad, T., Imran, S., Ismail, N.H., Selvaraj, M., Rahim, F., Chigurupati, S., Ullah, H., Khan, F., Salar, U., Javid, M.T., Vijayabalan, S., Khan, K.M., 2017. Biology-oriented drug synthesis (BIODS) of 2-(2-methyl-5-nitro-1*H*-imidazol-1-yl) ethyl aryl ether derivatives, *in vitro* α -amylase inhibitory activity and *in silico* studies. *Bioorg. Chem.* 74, 1–9.
- Ullah, S., Saeed, M., Halimi, S.M.A., Fakhri, M.I., Khan, K.M., Khan, I., Perveen, S., 2016. Piroxicam sulfonates biology-oriented drug synthesis (BIODS), characterization and anti-nociceptive screening. *Med. Chem. Res.* 25 (7), 1468–1475.
- Wahid, S., Jahangir, S., Versiani, M.A., Khan, K.M., Salar, U., Ashraf, M., Farzand, U., Wadood, A., Kanwal, A.-u.-R., Arshia, T.h., M., and Perveen, S., 2020. Atenolol thiourea hybrid as potent urease inhibitors: design, biology-oriented drug synthesis, inhibitory activity screening, and molecular docking studies. *Bioorg. Chem.* 94, 103359.
- Brito, C.D.L., Trossini, G.H.G., Ferreira, E.I., La-Scalea, M.A., 2013. Nitrofurazone and its nitroheterocyclic analogues: a study of the electrochemical behavior in aqueous medium. *J. Braz. Chem. Soc.* 24 (12), 1964–1973.
- Chin Chung, M., Longhin Bosquesi, P., Leandro dos Santos, J., 2011. A prodrug approach to improve the physico-chemical properties and decrease the genotoxicity of nitro compounds. *Curr. Pharm. Des.* 17 (32), 3515–3526.
- Blumenstiel, K., Schöneck, R., Yardley, V., Croft, S.L., Krauth-Siegel, R.L., 1999. Nitrofurans as common subversive substrates of *Trypanosoma cruzi* lipoamide dehydrogenase and trypanothione reductase. *Biochem. Pharmacol.* 58 (11), 1791–1799.
- Paulino, M., Iribarne, F., Dubin, M., Aguilera-Morales, S., Tapia, O., Stoppiani, A.O.M., 2005. The chemotherapy of Chagas' disease: an overview. *Mini Rev. Med. Chem.* 5 (5), 499–519.
- Chamberlain, R.E., 1976. Chemotherapeutic properties of prominent nitrofurans. *J. Antimicrob. Chemother.* 2, 325–336.
- Popiołek, L., Biernasiuk, A., 2016. Synthesis and investigation of antimicrobial activities of nitrofurazone analogues containing hydrazide-hydrazone moiety. *Saudi Pharm. J.* 25. <https://doi.org/10.1016/j.jsps.2017.05.006>.
- Taha, M., Imran, S., Ismail, N.H., Selvaraj, M., Rahim, F., Chigurupati, S., Ullah, H., Khan, F., Salar, U., Javid, M.T., Vijayabalan, S., Zaman, K., Khan, K.M., 2017. Biology-oriented drug synthesis (BIODS) of 2-(2-methyl-5-nitro-1*H*-imidazol-1-yl)ethyl aryl ether derivatives, *in vitro* α -amylase inhibitory activity and *in silico* studies. *Bioorg. Chem.* 74, 1–9.
- Khan, M., Alam, A., Khan, K.M., Salar, U., Chigurupati, S., Wadood, A., Ali, F., Mohammad, J.I., Riaz, M., Perveen, S., 2018. Flurbiprofen derivatives as novel α -amylase inhibitors: biology-oriented drug synthesis (BIODS), *in vitro*, and *in silico* evaluation. *Bioorg. Chem.* 81, 157–167.
- Gollapallia, M., Taha, M., Ullah, H., Nawaz, M., AlMuqarrabune, L. M.R., Rahim, F., Qureshi, F., Mossaddik, A., Ahmat, N., Khan, K. M., 2018. Synthesis of Bis-indolylmethane sulfonohydrazides derivatives as potent α -Glucosidase inhibitors. *Bioorg. Chem.* 80, 112–120.
- Abbasi, M.A., Shah, S.A.H., Aziz-ur-Rehman, Siddiqui, S.Z., Hussain, G., Khan, K.M., Ashraf, M., Ejaz, S.A. (2017). Synthesis of (*E*)-*N*'-[1-(2,4-dihydroxyphenyl)ethylidene]substituted hydrazides as possible α -glucosidase and butyrylcholinesterase inhibitors. *Journal of Chemical Society of Pakistan*, 39, 248-253.
- Tocher, J.H., 1997. Reductive activation of nitroheterocyclic compounds. *Gen. Pharmacol.* 28 (4), 485–487.
- Brondani, D.J., de Magalhaes Moreira, D.R., de Farias, M.P.A., Souza, F.R.D.S., Barbosa, F.F., Leite, A.C.L., 2007. A new and efficient N-alkylation procedure for semicarbazides/semicarbazones derivatives. *Tetrahedron Lett.* 48 (22), 3919–3923.
- Bartel, L.C., de Mecca, M.M., Castro, J.A., 2009. Nitroreductive metabolic activation of some carcinogenic nitro heterocyclic food contaminants in rat mammary tissue cellular fractions. *Food Chem. Toxicol.* 47 (1), 140–144.
- Solangi, M., Kanwal, Khan, K. M., Saleem, F., Hameed, S., Iqbal, J., Shafique, Z., Qureshi, U., Zaheer Ul-Haq, Taha, M., Perveen, S. (2020). Indole acrylonitriles as potential anti-hyperglycemic agents: Synthesis, α -glucosidase inhibitory activity and molecular docking studies. *Bioorganic & Medicinal Chemistry*, 28, 115605-115615.
- Chemical Computing Group (CCG) Inc. Molecular Operating Environment (MOE); Chemical Computing Group: Montreal, QC, Canada, 2019.
- Wang, J., Wolf, R. M., Caldwell, J.W., Kollman P.A., Case, D. A., 2004. Development and testing of a general amber force field. 25(9), 1157-1174.
- Wang, J., Wang, W., Kollman, P.A., Case, D.A., 2006. Automatic atom type and bond type perception in molecular mechanical calculations. *J. Mol. Graph. Model.* 25 (2), 247–260.
- Delano, W.L., 2010. The PyMOL molecular graphics system, Version 1.3 r1, Schrödinger, LLC, New York, pp. 1-10.
- Case, D., Ben-Shalom, I., Brozell, S., Cerutti, D., Cheatham, T., Cruzeiro, V., Darden, T., Duke, R., Ghoreishi, D., Gilson, M., 2018. AMBER 2018. University of California, San Francisco, California.
- Rehman, A.U., Rahman, M.U., Lu, S., Liu, H., Li, J.Y., Arshad, T., Wadood, A., Ng, H.L., Chen, H.F., 2020. Decoding allosteric communication pathways in protein lysine acetyltransferase. *Int. J. Biol. Macromol.* 149, 70–80.
- Rehman, A.U., Rafiq, H., Rahman, M.U., Li, J., Liu, H., Luo, S., Arshad, T., Wadood, A., Chen, H.F., 2019. Gain-of-function

- SHP2 E76Q mutant rescuing autoinhibition mechanism associated with juvenile myelomonocytic leukemia. *J. Chem. Inf. Model.* 59 (7), 3229–3239.
- Rehman, A.U., Khan, M.T., Liu, H., Wadood, A., Malik, S.I., Chen, H.F., 2019. Exploring the pyrazinamide drug resistance mechanism of clinical mutants T370P and W403G in ribosomal protein S1 of *Mycobacterium tuberculosis*. *J. Chem. Inf. Model.* 59 (4), 1584–1597.
- Rehman, A.U., Zhen, G., Zhong, B., Ni, D., Li, J., Nasir, A., Gabr, M.T., Rafiq, H., Wadood, A., Lu, S., Zhang, J., 2021. Mechanism of zinc ejection by disulfiram in nonstructural protein 5A. *PCCP*.
- Elahabaadi, E., Salarian, A.A., Nassireslami, E., 2021. Design, synthesis, and molecular docking of novel hybrids of coumarin-dithiocarbamate α -glucosidase inhibitors targeting type 2 diabetes mellitus. *Polycyclic Aromat. Compd.*, 1–11
- Zhang, L., Mchale, C.M., Greene, N., Snyder, R.D., Rich, I.N., Aardema, M.J., Roy, S., Pfuhrer, S., 2014. Commentary emerging approaches in predictive toxicology. *Environ. Mol. Mutagen.* 55, 679–688.
- Banerjee, P., Eckert, A.O., Schrey, A.K., Preissner, R., 2018. ProTox-II: a webserver for the prediction of toxicity of chemicals. *Nucleic Acids Res.* 46 (W1), W257–W263.
- Kroes, R., Renwick, A.G., Cheeseman, M., Kleiner, J., Mangelsdorf, I., Piersma, A., Schilter, B., Schlatter, J., van Schothorst, F., Vos, J. G., 2004. Structure-based thresholds of toxicological concern (TTC): guidance for application to substances present at low levels in the diet. *Food Chem. Toxicol.* 42, 65–83.